FRONTIERS OF PHYSICS

RESEARCH ARTICLE
Volume 18 / Issue 1 / 12304 / 2023

Unconventional photon blockade induced by the self-Kerr and cross-Kerr nonlinearities

Ling-Juan Feng[1,†], Li Yan[2,‡], Shang-Qing Gong[3,§]

1 School of Sciences, Shanghai Institute of Technology, Shanghai 201418, China
2 School of Physics and Electronic Engineering, Heze University, Heze 274015, China
3 School of Physics, East China University of Science and Technology, Shanghai 200237, China
Corresponding authors. E-mail: †lingjuanfeng@sit.edu.cn, ‡hzxyyl2014@163.com, §sqgong@ecust.edu.cn
Received April 16, 2022; accepted October 12, 2022

ABSTRACT

We study the use of the self-Kerr and cross-Kerr nonlinearities to realize strong photon blockade in a weakly driven, four-mode optomechanical system. According to the Born–Oppenheimer approximation, we obtain the cavity self-Kerr coupling and the inter-cavity cross-Kerr coupling, adiabatically separated from the mechanical oscillator. Through minimizing the second-order correlation function, we find out the optimal parameter conditions for the unconventional photon blockade. Under the optimal conditions, the strong photon blockade can appear in the strong or weak nonlinearities.

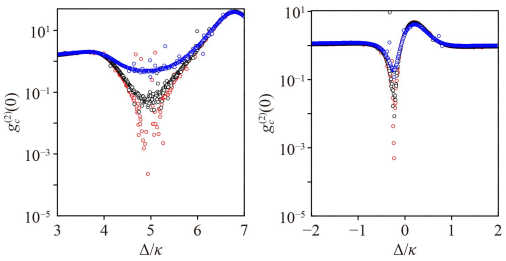

Keywords unconventional photon blockade, cross-Kerr nonlinearity, self-Kerr nonlinearity, optomechanical system

1 Introduction

Cavity optomechanics, based on the radiation-pressure coupling between light and mechanical oscillator, has attracted extensive attention in recent years [1– 3]. Thanks to this inherent nonlinear coupling, the optomechanical system provides a powerful platform to investigate the photon blockade. So far, there have been two methods for realizing the photon blockade, including the conventional photon blockade (CPB) and the unconventional photon blockade (UPB). The former arises due to the anharmonicity of the energy-level structure [4, 5]. Specifically, the resonant excitation of a single photon prevents the second or subsequent photons from simultaneous excitation. This phenomenon can be observed by evaluating the correlation function, which requires $g^{(2)}(0) < 1$ and $g^{(3)}(0) < 1$. However, to produce the sufficient anharmonicity, this scheme requires the strong nonlinear coupling between the cavity and mechanical modes. Therefore, some theoretical schemes have been proposed to significantly enhance the inherent nonlinear coupling, such as the postselected weak measurement [6], the delayed quantum feedback [7], the optical coalescence [8], the Josephson effect [9–11], and the squeezing effects of the cavity or mechanical mode [12–16].

In contrast, the realization of UPB only needs the weak Kerr nonlinearity in the system consisting of two coupled quantum boxes [17]. This arises from the destructive quantum interference between distinct excitation pathways [18], and satisfies the conditions $g^{(2)}(0) < 1$ and $g^{(3)}(0) > 1$. Based on this idea, the phenomenon of UPB has been observed in two coupled superconducting resonators [19] and quantum dot cavity-QED system [20]. Afterwards, it was studied in the three-mode optomechanical system, which contains two coupled optical modes and one mechanical mode [21–23].

We should note that most studies of CPB and UPB to date are based on the Kerr or Kerr-like nonlinearity. Different from these studies, Liao *et al.* [24, 25] used the cross-Kerr coupling between the cavity and mechanical

Higher Education Press

https://doi.org/10.1007/s11467-022-1213-y

modes to achieve the CPB effect. Also, Wang *et al.* [26] presented a scheme for implementing the UPB effect via the cross-Kerr coupling between two resonators. Recently, Yang *et al.* [27] found that the strong self-Kerr and cross-Kerr nonlinearities can significantly strengthen the CPB effect. Inspired by the above-mentioned works, in this paper, we are going to investigate the UPB with the self-Kerr and cross-Kerr nonlinearities in the multimode optomechanical system. This system can be considered as a four-mode system [28], in which two optical cavities are coupled to a mechanical oscillator and an auxiliary optical cavity via radiation pressure and photon tunneling, respectively. Under the Born–Oppenheimer (BO) approximation [28–31], two optical cavities are adiabatically separated from the mechanical oscillator, and the optomechanical parts simplify to the cavity self-Kerr and the inter-cavity cross-Kerr nonlinearities. Comparing with the previous work [27], the main novelty of our work is the realization of strong photon blockade in the condition of weak nonlinearity. Specifically, we calculate the equal-time second-order and third-order correlation functions, and then find that the UPB can be achieved for the strong or weak nonlinearities. Moreover, we briefly discuss the effect of pure dephasing on the UPB. Therefore, we hope that these results obtained will provide guidance for the implementation of strong photon blockades in the optomechanical systems.

2 Model and Hamiltonian

We consider a four-mode optomechanical system [28] as shown in Fig. 1(a). In this system, two optical modes a_1 and a_2 with frequencies ω_1 and ω_2 can couple with an auxiliary optical mode c with frequency ω_c via photon tunneling, and they are also coupled to one mechanical mode b with frequency ω_m by radiation pressure. To probe the photon blockade effect, we can drive the optical mode c using a monochromatic field with ω_d and Ω being the driving frequency and amplitude. In a rotating frame defined by $U(t)=\exp[-\mathrm{i}\omega_d t(a_1^\dagger a_1+a_2^\dagger a_2+c^\dagger c)]$, the system Hamiltonian is given by (setting $\hbar=1$)

$$\begin{aligned}H =&H_m+\Delta_1 a_1^\dagger a_1+\Delta_2 a_2^\dagger a_2+\Delta_c c^\dagger c+\Omega(c^\dagger+c)\\&+J_1(a_1^\dagger c+c^\dagger a_1)+J_2(a_2^\dagger c+c^\dagger a_2),\end{aligned}\tag{1}$$

where $H_m=\omega_m b^\dagger b+g_1 a_1^\dagger a_1(b^\dagger+b)+g_2 a_2^\dagger a_2(b^\dagger+b)$ describes the mechanical part. a_1 ($a_1^\dagger$), a_2 ($a_2^\dagger$), and c ($c^\dagger$) represent the photon annihilation (creation) operators for the optical modes. Similarly, b ($b^\dagger$) denotes the phonon annihilation (creation) operator of the mechanical mode. The last two terms in Eq. (1) correspond to the photon tunneling interaction between the two optical and the auxiliary optical modes with the tunneling coupling strengths J_1 and J_2. The second and third terms in H_m are the radiation pressure interaction between the optical and mechanical modes with the optomechanical coupling strengths g_1 and g_2 [32]. $\Delta_k=\omega_k-\omega_d$ $(k=1,2,c)$ is the detuning of the optical field from the driving field. Here, by adjusting the driving frequency ω_d, the detuning Δ_k can be much smaller than the mechanical frequency ω_m. With this condition, the optical and mechanical mode can be considered as the slow and fast variables, respectively, and the BO approximation can be applied to H_m [28–31].

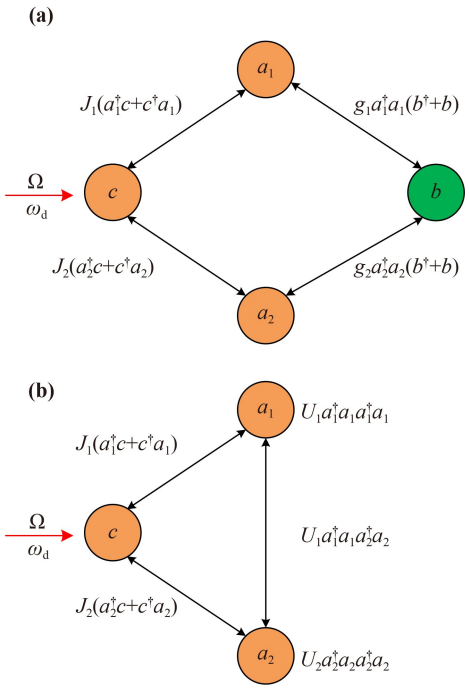

Fig. 1 **(a)** Schematic diagram of the four-mode optomechanical system, with three optical modes and a single mechanical mode. **(b)** Schematic diagram of the three-coupled-cavity system.

Introducing the mechanical position and momentum operators with m_{eff} being the effective mass, $x=\sqrt{\frac{1}{2m_{\mathrm{eff}}\omega_m}}(b^\dagger+b)$ and $p=\mathrm{i}\sqrt{\frac{m_{\mathrm{eff}}\omega_m}{2}}(b^\dagger-b)$, H_m can be rewritten as

$$\begin{aligned}H_m=&\frac{p^2}{2m_{\mathrm{eff}}}+\frac{m_{\mathrm{eff}}\omega_m^2 x^2}{2}+\sqrt{2m_{\mathrm{eff}}\omega_m}(g_1 a_1^\dagger a_1+g_2 a_2^\dagger a_2)x\\=&\frac{p^2}{2m_{\mathrm{eff}}}+\frac{m_{\mathrm{eff}}\omega_m^2}{2}\left[x+\sqrt{\frac{2}{m_{\mathrm{eff}}\omega_m^3}}(g_1 a_1^\dagger a_1+g_2 a_2^\dagger a_2)\right]^2\\&-\frac{(g_1 a_1^\dagger a_1+g_2 a_2^\dagger a_2)^2}{\omega_m}\\=&\frac{p^2}{2m_{\mathrm{eff}}}+\frac{m_{\mathrm{eff}}\omega_m^2 X^2}{2}-\frac{(g_1 a_1^\dagger a_1+g_2 a_2^\dagger a_2)^2}{\omega_m}\\=&\omega_m A^\dagger A-U_1 a_1^\dagger a_1 a_1^\dagger a_1-U_2 a_2^\dagger a_2 a_2^\dagger a_2-U a_1^\dagger a_1 a_2^\dagger a_2,\end{aligned}\tag{2}$$

where we have used the BO adiabatic separation between the the optical and mechanical modes. $A=\sqrt{\frac{m_{\mathrm{eff}}\omega_m}{2}}\left(X+\frac{\mathrm{i}p}{m_{\mathrm{eff}}\omega_m}\right)$ and $X=x+\sqrt{\frac{2}{m_{\mathrm{eff}}\omega_m^3}}(g_1 a_1^\dagger a_1+$

$g_2 a_2^\dagger a_2$) are the annihilation and displacement operators. $U_k = \frac{g_k^2}{\omega_m}$ and $U = \frac{2g_1 g_2}{\omega_m}$ are the self- and cross-Kerr nonlinear coefficients. By tracing the Hamiltonian (1) over the mechanical space, we obtain the reduced Hamiltonian for the pure optical system

$$\begin{aligned} H_{\text{eff}} =& \text{Tr}[H|m\rangle\langle m|] \\ =& \Delta_1 a_1^\dagger a_1 + \Delta_2 a_2^\dagger a_2 + \Delta_c c^\dagger c + \Omega(c^\dagger + c) \\ &+ J_1(a_1^\dagger c + c^\dagger a_1) + J_2(a_2^\dagger c + c^\dagger a_2) \\ &- U_1 a_1^\dagger a_1 a_1^\dagger a_1 - U_2 a_2^\dagger a_2 a_2^\dagger a_2 - U a_1^\dagger a_1 a_2^\dagger a_2, \end{aligned} \tag{3}$$

where the mechanical energy $m\omega_m$ has been removed by resetting the ground energy, and $|m\rangle$ is the mechanical eigenvector. From the above Hamiltonian, our model can be considered as a three-coupled-cavity system [see Fig. 1(b)] and also indicates that the self-Kerr nonlinearity of the cavity mode and the cross-Kerr nonlinearity between the optical modes are induced by the BO adiabatic separation between the optical and mechanical modes.

3 Results and discussion

In the following, we will investigate the impact of the self- and cross-Kerr nonlinearities on the unconventional photon blockade (UPB) in the mode c, and check the validity of the effective Hamiltonian H_{eff}. Usually, the UPB effect can be studied by analyzing the equal-time second-order and third-order correlation functions in the steady state, i.e., $g_c^{(\mu)}(0) = \lim_{t\to\infty} \frac{\langle c^{\dagger\mu} c^\mu\rangle(t)}{\langle c^\dagger c\rangle^\mu(t)}$ for $\mu = 2, 3$. The values of $g_c^{(2)}(0) < 1$ and $g_c^{(3)}(0) > 1$, manifesting two-photon antibunching and three-photon bunching, indicates that UPB only blocks the emission of two photons, but simultaneously allows the emission of three photons.

Specifically, the equal-time second-order correlation function $g_c^{(2)}(0)$ can be analytically calculated from the non-Hermitian Schrödinger equation. Here, we phenomenologically introduce the optical decay to H_{eff}, and then obtain the non-Hermitian Hamiltonian

$$H_{\text{non}} = H_{\text{eff}} - \frac{i\kappa_1}{2} a_1^\dagger a_1 - \frac{i\kappa_2}{2} a_2^\dagger a_2 - \frac{i\kappa_c}{2} c^\dagger c, \tag{4}$$

where κ_k $(k = 1, 2, c)$ is the decay rate. In the weak-driving regime, i.e., $\Omega \ll \kappa_c$, by truncating the optical space to $n_{a_1} + n_{a_2} + n_c \leqslant 2$, the state of this optical system can be written as

$$\begin{aligned} |\psi\rangle =& C_{000}|000\rangle + C_{001}|001\rangle + C_{100}|100\rangle + C_{010}|010\rangle \\ &+ C_{002}|002\rangle + C_{101}|101\rangle + C_{011}|011\rangle + C_{110}|110\rangle \\ &+ C_{200}|200\rangle + C_{020}|020\rangle, \end{aligned} \tag{5}$$

with the probability amplitudes $C_{n_{a_1} n_{a_2} n_c}$. Then we substitute the non-Hermitian Hamiltonian (4) and the state (5) into the Schrödinger equation $i\frac{d|\psi\rangle}{dt} = H_{\text{non}}|\psi\rangle$ to obtain the evolution equations of the coefficients $C_{n_{a_1} n_{a_2} n_c}$, which reads

$$\begin{aligned} i\dot{C}_{000} =& \Omega C_{001}, \\ i\dot{C}_{001} =& \Omega C_{000} + \sqrt{2}\Omega C_{002} + J(C_{100} + C_{010}) \\ &+ (\Delta - i\kappa/2) C_{001}, \\ i\dot{C}_{100} =& \Omega C_{101} + J C_{001} + (\Delta - i\kappa/2 - U/2) C_{100}, \\ i\dot{C}_{010} =& \Omega C_{011} + J C_{001} + (\Delta - i\kappa/2 - U/2) C_{010}, \\ i\dot{C}_{002} =& \sqrt{2}\Omega C_{001} + \sqrt{2} J(C_{101} + C_{011}) + 2(\Delta - i\kappa/2) C_{002}, \\ i\dot{C}_{101} =& \Omega C_{100} + \sqrt{2} J(C_{002} + C_{200}) + J C_{110} \\ &+ 2(\Delta - i\kappa/2 - U/4) C_{101}, \\ i\dot{C}_{011} =& \Omega C_{010} + \sqrt{2} J(C_{002} + C_{020}) + J C_{110} \\ &+ 2(\Delta - i\kappa/2 - U/4) C_{011}, \\ i\dot{C}_{110} =& J(C_{011} + C_{101}) + 2(\Delta - i\kappa/2 - U) C_{110}, \\ i\dot{C}_{200} =& \sqrt{2} J C_{101} + 2(\Delta - i\kappa/2 - U) C_{200}, \\ i\dot{C}_{020} =& \sqrt{2} J C_{011} + 2(\Delta - i\kappa/2 - U) C_{020}, \end{aligned} \tag{6}$$

where we simply consider $\Delta_k = \Delta$, $\kappa_k = \kappa$, $J_1 = J_2 = J$, and $g_1 = g_2 = g$. By neglecting higher-order term in each equation, we can approximately solve these equations in Eq. (6), and then obtain the steady-state solutions of the coefficients $C_{n_{a_1} n_{a_2} n_c}$:

$$\begin{aligned} C_{000} =& 1, \\ C_{001} =& -2(U - 2\Delta + i\kappa)\Omega/M, \\ C_{100} =& C_{010} = -4J\Omega/M, \\ C_{002} =& 2\sqrt{2}[8J^2 U + (U - 2\Delta + i\kappa)(2U - 2\Delta + i\kappa) \\ &\cdot (U - 4\Delta + 2i\kappa)]\Omega^2/N, \\ C_{101} =& C_{011} = 8J(2U - 2\Delta + i\kappa)(U - 4\Delta + 2i\kappa)\Omega^2/N, \\ C_{110} =& 16J^2(U - 4\Delta + 2i\kappa)\Omega^2/N, \\ C_{200} =& C_{020} = C_{110}/\sqrt{2}, \end{aligned} \tag{7}$$

with

$$\begin{aligned} M =& 8J^2 + (2\Delta - i\kappa)(U - 2\Delta + i\kappa), \\ N =& M[16J^2(U - 2\Delta + i\kappa) + (2\Delta - i\kappa)(2U - 2\Delta + i\kappa) \\ &\cdot (U - 4\Delta + 2i\kappa)]. \end{aligned} \tag{8}$$

For the weak-driving case, we have the approximate solutions, $\{C_{002}, C_{101}, C_{011}, C_{110}, C_{200}, C_{020}\} \sim \Omega^2$ and $\{C_{001}, C_{100}, C_{010}\} \sim \Omega$. Hence, the second-order correlation function is given by

$$\begin{aligned} g_c^{(2)}(0) &= \frac{2|C_{002}|^2}{(|C_{001}|^2 + |C_{101}|^2 + |C_{011}|^2 + 2|C_{002}|^2)^2} \\ &\approx \frac{2|C_{002}|^2}{|C_{001}|^4}. \end{aligned} \tag{9}$$

Following the similar method as above, the third-order correlation function is

$$g_c^{(3)}(0) \approx \frac{6|C_{003}|^2}{|C_{001}|^6}, \tag{10}$$

where

$$\begin{aligned} C_{003} =& -512\sqrt{2/3}J^4[18U^2-8(2\Delta-\mathrm{i}\kappa)^2+U(-6\Delta+3\mathrm{i}\kappa)] \\ & \cdot(3U-2\Delta+\mathrm{i}\kappa)\Omega^3/G+32\sqrt{2/3}J^2U[104U^3 \\ & +304U(2\Delta-\mathrm{i}\kappa)^2-71(2\Delta-\mathrm{i}\kappa)^3 \\ & +361U^2(-2\Delta+\mathrm{i}\kappa)](4U-6\Delta+3\mathrm{i}\kappa)\Omega^3/G \\ & +36\sqrt{2/3}(U-2\Delta+\mathrm{i}\kappa)(2U-2\Delta+\mathrm{i}\kappa) \\ & \cdot(3U-2\Delta+\mathrm{i}\kappa)(U-4\Delta+2\mathrm{i}\kappa)(U-6\Delta+3\mathrm{i}\kappa) \\ & \cdot(4U-6\Delta+3\mathrm{i}\kappa)^2\Omega^3/G \\ & +2048\sqrt{2/3}J^6(U+4\Delta-2\mathrm{i}\kappa)\Omega^3/G, \end{aligned} \tag{11}$$

with

$$\begin{aligned} G =& -8J^2N[36U^2+27(2\Delta-\mathrm{i}\kappa)^2+77U(-2\Delta+\mathrm{i}\kappa)] \\ & \cdot(4U-6\Delta+3\mathrm{i}\kappa)-3N(2\Delta-\mathrm{i}\kappa)(3U-2\Delta+\mathrm{i}\kappa) \\ & \cdot(U-6\Delta+3\mathrm{i}\kappa)(4U-6\Delta+3\mathrm{i}\kappa)^2 \\ & +512NJ^4(U-2\Delta+\mathrm{i}\kappa). \end{aligned} \tag{12}$$

According to the analytical expression for the second-order correlation function (9), if $C_{002}=0$, then $g_c^{(2)}(0)\to 0$. In this case, the photons will exhibit the nearly perfect antibunching, indicating the appearance of complete photon blockade. Therefore, we obtain the optimal conditions for the unconventional photon blockade (UPB) in the mode c as

$$\begin{aligned} 0 =& 8J^2U+2U^3-14U^2\Delta+28U\Delta^2-16\Delta^3 \\ & -7U\kappa^2+12\Delta\kappa^2, \\ 0 =& 7U^2\kappa-28U\Delta\kappa+24\Delta^2\kappa-2\kappa^3. \end{aligned} \tag{13}$$

For fixed J and κ, the optimal parameters Δ_{opt} and U_{opt} can be obtained from the above equations. However, these results are too cumbersome to be given here. Figure 2 displays the optimal parameters $\Delta_{\mathrm{opt}}/\kappa$ and U_{opt}/κ as functions of normalized photon tunneling J/κ. Obviously, there are two sets of optimal parameters, and they are valid for $J/\kappa>0.68$. In Fig. 2(a), the optimal nonlinearity U_{opt}/κ (i.e., the optimal self- or cross-Kerr nonlinearity) increases with increasing photon tunneling J/κ, but in Fig. 2(b), the optimal nonlinearity U_{opt}/κ decreases with increasing J/κ. This implies that the strong or weak nonlinearity could lead to the complete photon blockade.

Qualitatively, the origin of complete photon blockade can be understood from quantum interference effect, as shown in Fig. 3. The interference can happen between the three different paths for two-photon excitation: the direct excitation from $|001\rangle \xrightarrow{\Omega} |002\rangle$, and the two tunnel-coupling-mediated transitions $|011\rangle \xrightarrow{J} |002\rangle$ and $|101\rangle \xrightarrow{J} |002\rangle$. If the parameters Δ and U can satisfy the optimal conditions (13), the three different excitation paths will destructively interfere, resulting in the complete suppression of two-photon excitation. Apparently, these remarkable features are attributed to the UPB effect.

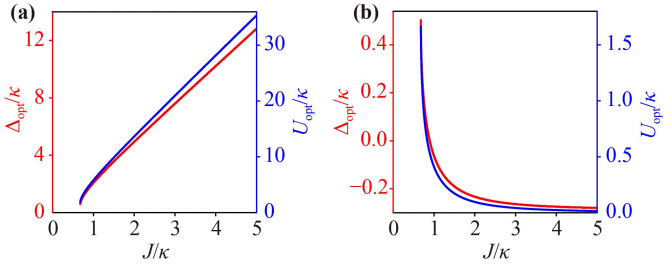

Fig. 2 **(a)** One set of optimal detuning Δ_{opt} and nonlinearity U_{opt} versus photon tunneling J normalized to κ. **(b)** Another set of optimal detuning Δ_{opt} and nonlinearity U_{opt} versus photon tunneling J normalized to κ.

To further verify the analytical results $g_c^{(2)}(0)$ and $g_c^{(3)}(0)$, we numerically study the quantum dynamics of the present system. We introduce the Lindblad master equation of the density operator ρ for the driven-dissipative system,

$$\begin{aligned} \dot{\rho} =& -\mathrm{i}[H,\rho]+\frac{\kappa_1}{2}L[a_1]\rho+\frac{\kappa_2}{2}L[a_2]\rho+\frac{\kappa_c}{2}L[c]\rho \\ & +\frac{\gamma}{2}N_{\mathrm{th}}L[b^\dagger]\rho+\frac{\gamma}{2}(N_{\mathrm{th}}+1)L[b]\rho, \end{aligned} \tag{14}$$

where the Hamiltonian H is given by Eq. (1) or Eq. (3), $L[o]\rho=2o\rho o^\dagger-o^\dagger o\rho-\rho o^\dagger o$ $(o=a_1,a_2,c,b,b^\dagger)$ is the Lindblad superoperator for the three optical modes and the mechanical mode, κ_k and γ denote the decay rate of the cavity fields $(k=1,2,c)$ and the damping rate of the mechanical oscillator, respectively. $N_{\mathrm{th}}=[\exp(\hbar\omega_m/(k_BT))-1]^{-1}$ is the thermal phonon number in the mechanical mode with the environmental temperature T and the Boltzmann constant k_B. Here, the steady-state value of $g_c^{(2)}(0)$ and $g_c^{(3)}(0)$ can be obtained by numerically simulating the Lindblad master equation (14) and from the density matrix operator in the steady state as $g_c^{(\mu)}(0)=\frac{\mathrm{Tr}(\rho c^{\dagger\mu}c^\mu)}{[\mathrm{Tr}(\rho c^\dagger c)]^\mu}$ with $\mu=2,3$.

Next, we numerically check the validity of the approximation from the full Hamiltonian (1) to the effective Hamiltonian (3). In Fig. 4, we show the evolution of the second-order correlation function $g_c^{(2)}(0)$ with the Hamiltonians H and H_{eff} as a function of the scaled time κt.

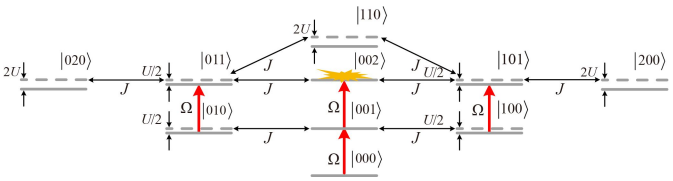

Fig. 3 Energy-level diagram of the optical system under the Hamiltonian (3) with $J_1=J_2=J$ and $g_1=g_2=g$. States are labeled $|n_{a_1}n_{a_2}n_c\rangle$, where n_j denotes the photon number of the mode $j=a_1,a_2,c$.

The values of Δ and U are considered to be the optimal parameters $\Delta_{\rm opt}$ and $U_{\rm opt}$. When the photon tunneling $J=2\kappa$, $\Delta_{\rm opt}$ and $U_{\rm opt}$ from Eq. (13) are calculated as follows: $\Delta_{\rm opt}\approx 4.934\kappa$ and $U_{\rm opt}\approx 13.637\kappa$; $\Delta_{\rm opt}\approx -0.233\kappa$ and $U_{\rm opt}\approx 0.096\kappa$. By comparing the numerical results $g_c^{(2)}(0)$ under two sets of optimal parameters, we find that there are no significant differences between them. From Fig. 4, it is evident that the approximate results corresponding to the effective Hamiltonian $H_{\rm eff}$ are in excellent agreement with the exact results using the full Hamiltonian H. We also note that when $\kappa t=15$, the correlation function $g_c^{(2)}(0)$ approaches a steady value 10^{-4}. For the decay rate of the cavity mode $\kappa=0.1$ MHz, the corresponding relaxation time is $t\approx 150$ μs.

In view of rapid progress of optomechanical technology, we find that our system is also possibly realized in the multimode optomechanical system [33, 34]. To further obtain the pure optical system, we use the mechanical frequency $\omega_m=10^2\kappa$ for the realization of the BO approximation. Currently, several optomechanical systems, such as photonic and phononic crystals [35] or microtoroid [36], have the high-frequency mechanical modes (on the order of ~ MHz–GHz), so that the condition of the BO approximation is satisfied. For observation of the UPB effect, we need to satisfy the optimal condition, namely the strong or weak nonlinearity U (i.e., optomechanical coupling g). However, except for cold-atomic experiments [37, 38], the strong nonlinear coupling in the optomechanical experiments is not so easy to realize. To achieve strong coupling, it has been suggested theoretically to use the coalescence effect [8], the Josephson effect [9–11], the squeezing effect [12–16], and so on. These methods could significantly enhance coupling strength by several orders of magnitude. Thus, our used parameters could be implemented in the currently available optomechanical systems.

Figure 5 plots the second-order correlation function $g_c^{(2)}(0)$ as a function of Δ/κ for different values U. Here, we observe the difference between the numerical and the analytical results for $g_c^{(2)}(0)$. This is because the Hilbert space of the optical system can be truncated to the finite dimension. Specifically, in the approximate analytical calculation, we can truncate the photon state according to the low-excitation number $n_{a_1}+n_{a_2}+n_c\leqslant 2$. However, in the numerical simulation, we have taken into account the higher state for $n_{a_1}+n_{a_2}+n_c\geqslant 3$. In Figs. 5(a) and (b), for the photon tunneling $J=2\kappa$, the optimal nonlinearities are $U_{\rm opt}\approx 13.637\kappa$ and $U_{\rm opt}\approx 0.096\kappa$ that correspond to the optimal detunings of $\Delta_{\rm opt}\approx 4.934\kappa$ and $\Delta_{\rm opt}\approx -0.233\kappa$, respectively. These optimal values are calculated analytically according to Eq. (13). As expected, $g_c^{(2)}(0)$ reaches the minimal value 10^{-4} at the optimal detuning $\Delta_{\rm opt}$, and shows strong photon blockade in the strong- or weak-coupling regime. On the other hand, when we consider the case of vanishing nonlinearity ($U=0$), we find $g_c^{(2)}(0)\to 1$, i.e., there is no photon blockade effect. Therefore, the nonlinearity is necessary for generating photon blockade.

To more clearly visualize photon blockade, we show the second- and third-order correlation functions $g_c^{(2)}(0)$ and $g_c^{(3)}(0)$ as functions of Δ/κ. From Figs. 6(a) and (b), whether in the strong-coupling regime ($U>\kappa$) or in the weak-coupling regime ($U<\kappa$), we can observe $g_c^{(2)}(0)<1$ and $g_c^{(3)}(0)>1$ around the optimum value $\Delta_{\rm opt}$, which indicates that two-photon emission is suppressed but three-photon emission is enhanced. It should be noted that this phenomenon corresponds to the UPB effect, coming from the destructive quantum interference.

Finally, we study the influence of pure dephasing on the UPB effect [22, 39]. To illustrate how the pure dephasing affects UPB, we introduce another Lindblad term defined by $\frac{\gamma_p}{2}L[c^\dagger c]\rho$ into the master equation (14), where γ_p is the pure dephasing rate of the cavity mode c. In Figs. 7(a) and (b), we plot the second-order correlation function $g_c^{(2)}(0)$ as a function of Δ/κ for different pure-dephasing rates $\gamma_p=0$, $\gamma_p=0.01\kappa$, $\gamma_p=0.1\kappa$. It can be seen that with the increase of the pure-dephasing rate,

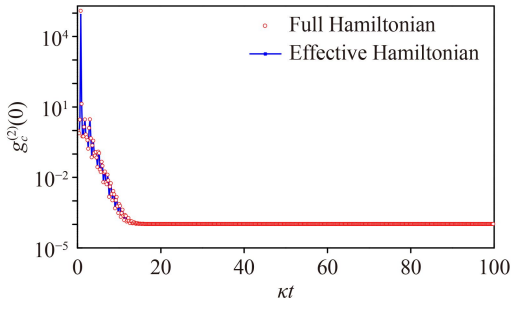

Fig. 4 The second-order correlation function $g_c^{(2)}(0)$ versus the time κt. The red circles show the exact numerical results based on the full Hamiltonian (1) and the master equation (14). The solid blue curve is the approximate numerical results based on the effective Hamiltonian (3) and the master equation (14). The parameters are $J=2\kappa$, $\Delta=\Delta_{\rm opt}$, $U=U_{\rm opt}$, $\omega_m=10^2\kappa$, $N_{\rm th}=0$, $\gamma=10^{-3}\kappa$, and $\Omega=10^{-2}\kappa$.

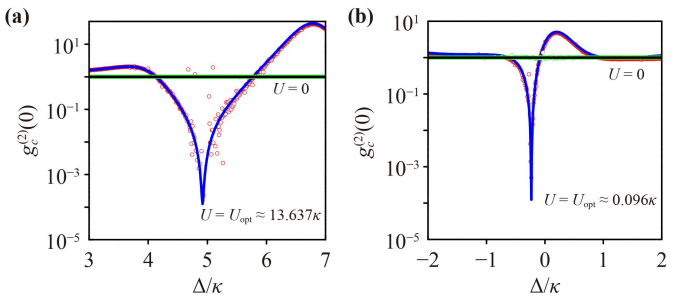

Fig. 5 The second-order correlation function $g_c^{(2)}(0)$ versus the normalized detuning Δ/κ for different values of the nonlinearity U. The red (or green) circles denote the numerical results based on Eqs. (3) and (14). The solid blue (or black) curve is the analytical results based on Eq. (9). Other parameters are the same as those in Fig. 4.

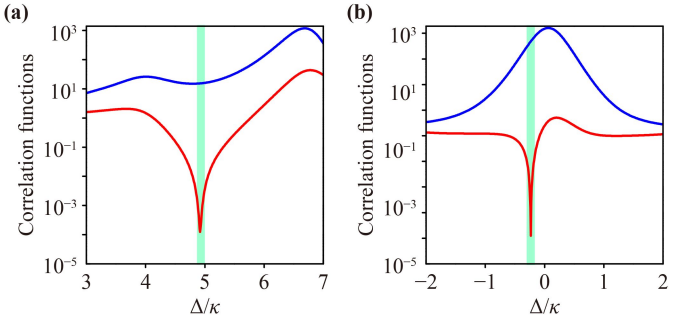

Fig. 6 The second- and third-order correlation functions $g_c^{(2)}(0)$ and $g_c^{(3)}(0)$ versus the normalized detuning Δ/κ. The solid red curve corresponds to the analytical results of $g_c^{(2)}(0)$ based on Eq. (9). The solid blue curve is the analytical results of $g_c^{(3)}(0)$ based on Eq. (10). In (a) $U_{\rm opt} \approx 13.637\kappa$ and in (b) $U_{\rm opt} \approx 0.096\kappa$. Other parameters are the same as those in Fig. 4.

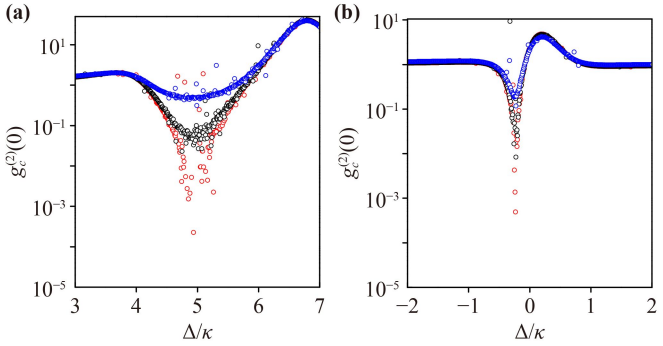

Fig. 7 The second-order correlation function $g_c^{(2)}(0)$ versus the normalized detuning Δ/κ for different values of the pure dephasing rate γ_p. These circles show the numerical results based on Eqs. (3) and (14). The red, black, blue circles respectively represent $\gamma_p = 0$, $\gamma_p = 0.01\kappa$, $\gamma_p = 0.1\kappa$. In **(a)** $U_{\rm opt} \approx 13.637\kappa$ and in **(b)** $U_{\rm opt} \approx 0.096\kappa$. Other parameters are the same as those in Fig. 4.

$g_c^{(2)}(0)$ increases gradually at the optimal detuning ($\Delta_{\rm opt} \approx 4.934\kappa$ or $\Delta_{\rm opt} \approx -0.233\kappa$). This means that the strong pure dephasing can attenuate the UPB effect, leading to the weak photon antibunching.

4 Conclusion

In summary, we have analyzed the unconventional photon blockade effect (UPB) in the four-mode optomechanical system. In this system, the self- and cross-Kerr nonlinearities result from the BO adiabatic separation between the optical and mechanical modes, which is the important factor to produce the UPB effect. By minimizing the result of the second-order correlation function, we derive the two sets of the optimal parameter conditions required for the UPB. It is found that under these conditions, the UPB can be observed in the strong or weak nonlinearities. This is due to the destructive quantum interference between the three different paths for two-photon excitation in the mode c. Additionally, we also find that the pure dephasing has an undesirable effect on the UPB.

Acknowledgements This work was supported by the National Natural Science Foundation of China (Grant Nos. 12034007 and 12204310), the Shanghai Sailing Program (Grant No. 21YF1446900), and the Research start-up project of Shanghai Institute of Technology (Grant No. YJ2021-65).

References

1. T. J. Kippenberg and K. J. Vahala, Cavity optomechanics: Back-action at the mesoscale, *Science* 321(5893), 1172 (2008)
2. M. Aspelmeyer, P. Meystre, and K. Schwab, Quantum optomechanics, *Phys. Today* 65(7), 29 (2012)
3. M. Aspelmeyer, T. J. Kippenberg, and F. Marquardt, Cavity optomechanics, *Rev. Mod. Phys.* 86(4), 1391 (2014)
4. P. Rabl, Photon blockade effect in optomechanical systems, *Phys. Rev. Lett.* 107(6), 063601 (2011)
5. A. Nunnenkamp, K. Børkje, and S. M. Girvin, Single-photon optomechanics, *Phys. Rev. Lett.* 107(6), 063602 (2011)
6. G. Li, T. Wang, and H. S. Song, Amplification effects in optomechanics via weak measurements, *Phys. Rev. A* 90(1), 013827 (2014)
7. Z. Y. Wang and A. H. Safavi-Naeini, Enhancing a slow and weak optomechanical nonlinearity with delayed quantum feedback, *Nat. Commun.* 8(1), 15886 (2017)
8. C. Genes, A. Xuereb, G. Pupillo, and A. Dantan, Enhanced optomechanical readout using optical coalescence, *Phys. Rev. A* 88(3), 033855 (2013)
9. T. T. Heikkilä, F. Massel, J. Tuorila, R. Khan, and M. A. Sillanpää, Enhancing optomechanical coupling via the Josephson effect, *Phys. Rev. Lett.* 112(20), 203603 (2014)
10. J. M. Pirkkalainen, S. U. Cho, F. Massel, J. Tuorila, T. T. Heikkilä, P. J. Hakonen, and M. A. Sillanpää, Cavity optomechanics mediated by a quantum two-level system, *Nat. Commun.* 6(1), 6981 (2015)
11. D. Bothner, I. C. Rodrigues, and G. A. Steele, Photon-pressure strong coupling between two superconducting circuits, *Nat. Phys.* 17(1), 85 (2021)
12. X. Y. Lü, Y. Wu, J. R. Johansson, H. Jing, J. Zhang, and F. Nori, Squeezed optomechanics with phase-matched amplification and dissipation, *Phys. Rev. Lett.* 114(9), 093602 (2015)
13. M. A. Lemonde, N. Didier, and A. A. Clerk, Enhanced nonlinear interactions in quantum optomechanics via mechanical amplification, *Nat. Commun.* 7(1), 11338 (2016)
14. T. S. Yin, X. Y. Lü, L. L. Zheng, M. Wang, S. Li, and Y. Wu, Nonlinear effects in modulated quantum optomechanics, *Phys. Rev. A* 95(5), 053861 (2017)
15. L. J. Feng and S. Q. Gong, Two-photon blockade generated

and enhanced by mechanical squeezing, *Phys. Rev. A* 103(4), 043509 (2021)
16. D. L. Chen, Y. H. Chen, Y. Liu, Z. C. Shi, J. Song, and Y. Xia, Detecting a single atom in a cavity using the χ(2) nonlinear medium, *Front. Phys.* 17(5), 52501 (2022)
17. T. C. H. Liew and V. Savona, Single photons from coupled quantum modes, *Phys. Rev. Lett.* 104(18), 183601 (2010)
18. M. Bamba, A. Imamoğlu, I. Carusotto, and C. Ciuti, Origin of strong photon antibunching in weakly nonlinear photonic molecules, *Phys. Rev. A* 83(2), 021802(R) (2011)
19. C. Vaneph, A. Morvan, G. Aiello, M. Féchant, M. Aprili, J. Gabelli, and J. Estéve, Observation of the unconventional photon blockade in the microwave domain, *Phys. Rev. Lett.* 121(4), 043602 (2018)
20. H. J. Snijders, J. A. Frey, J. Norman, H. Flayac, V. Savona, A. C. Gossard, J. E. Bowers, M. P. van Exter, D. Bouwmeester, and W. Löffler, Observation of the unconventional photon blockade, *Phys. Rev. Lett.* 121(4), 043601 (2018)
21. X. W. Xu and Y. J. Li, Antibunching photons in a cavity coupled to an optomechanical system, *J. Phys. At. Mol. Opt. Phys.* 46(3), 035502 (2013)
22. B. Sarma and A. K. Sarma, Unconventional photon blockade in three-mode optomechanics, *Phys. Rev. A* 98(1), 013826 (2018)
23. D. Y. Wang, C. H. Bai, S. T. Liu, S. Zhang, and H. F. Wang, Photon blockade in a double-cavity optomechanical system with nonreciprocal coupling, *New J. Phys.* 22(9), 093006 (2020)
24. F. Zou, L. B. Fan, J. F. Huang, and J. Q. Liao, Enhancement of few-photon optomechanical effects with cross-Kerr nonlinearity, *Phys. Rev. A* 99(4), 043837 (2019)
25. J. Q. Liao, J. F. Huang, L. Tian, L. M. Kuang, and C. P. Sun, Generalized ultrastrong optomechanical-like coupling, *Phys. Rev. A* 101(6), 063802 (2020)
26. Y. M. Wang, G. Q. Zhang, and W. L. You, Photon blockade with cross-Kerr nonlinearity in superconducting circuits, *Laser Phys. Lett.* 15(10), 105201 (2018)
27. J. Y. Yang, Z. Yang, C. S. Zhao, R. Peng, S. L. Chao, and L. Zhou, Nonlinearity enhancement and photon blockade in hybrid optomechanical systems, *Opt. Express* 29(22), 36167 (2021)
28. Y. B. Qian, D. G. Lai, M. R. Chen, and B. P. Hou, Nonreciprocal photon transmission with quantum noise reduction via cross-Kerr nonlinearity, *Phys. Rev. A* 104(3), 033705 (2021)
29. Z. R. Gong, H. Ian, Y. X. Liu, C. P. Sun, and F. Nori, Effective Hamiltonian approach to the Kerr nonlinearity in an optomechanical system, *Phys. Rev. A* 80(6), 065801 (2009)
30. N. Imoto, H. A. Haus, and Y. Yamamoto, Quantum nondemolition measurement of the photon number via the optical Kerr effect, *Phys. Rev. A* 32(4), 2287 (1985)
31. D. F. Walls and G. J. Milburn, Quantum Optics, Springer-Verlag, Berlin, 1994
32. C. K. Law, Interaction between a moving mirror and radiation pressure: A Hamiltonian formulation, *Phys. Rev. A* 51(3), 2537 (1995)
33. F. Ruesink, M. Miri, A. Alù, and E. Verhagen, Nonreciprocity and magnetic-free isolation based on optomechanical interactions, *Nat. Commun.* 7(1), 13662 (2016)
34. N. R. Bernier, L. D. Tóth, A. Koottandavida, M. A. Ioannou, D. Malz, A. Nunnenkamp, A. K. Feofanov, and T. J. Kippenberg, Nonreciprocal reconfigurable microwave optomechanical circuit, *Nat. Commun.* 8(1), 604 (2017)
35. M. Eichenfield, J. Chan, R. M. Camacho, K. J. Vahala, and O. Painter, Optomechanical crystals, *Nature* 462(7269), 78 (2009)
36. A. Schliesser, R. Rivière, G. Anetsberger, O. Arcizet, and T. J. Kippenberg, Resolved-sideband cooling of a micromechanical oscillator, *Nat. Phys.* 4, 415 (2008)
37. S. Gupta, K. L. Moore, K. W. Murch, and D. M. Stamper-Kurn, Cavity nonlinear optics at low photon numbers from collective atomic motion, *Phys. Rev. Lett.* 99(21), 213601 (2007)
38. F. Brennecke, S. Ritter, T. Donner, and T. Esslinger, Cavity optomechanics with a Bose–Einstein condensate, *Science* 322(5899), 235 (2008)
39. B. Sarma and A. K. Sarma, Quantum-interference-assisted photon blockade in a cavity via parametric interactions, *Phys. Rev. A* 96(5), 053827 (2017)